Waveform inversion including well constraints, anisotropy, and attenuation

CHAO WANG, DAVID YINGST, JIANYONG BAI, JACQUES LEVEILLE, PAUL FARMER, and JOHN BRITTAN, ION Geophysical

The goal of full-waveform inversion (WFI) is to derive high-fidelity Earth models for seismic imaging from the full waveforms of the acquired seismic data. The attractiveness of WFI lies mainly in its limited number of approximations, at least in a theoretical sense, in contrast to other model determination techniques such as semblance or ray-based tomography. Despite this, various methodologies must be utilized to make the technique viable with today's computing technology and restrictions of seismic acquisition. These are collectively referred to as "waveform-inversion strategies" and in this article we discuss mainly regularization and preconditioning strategies. As the wavefields need to be accurately modeled to represent the kinematics of all the waves during WFI iterations, the inclusion of anisotropy often helps to improve the WFI results. In the first section of this article, we introduce forward modeling and its adjoint based on acoustic-wave equations in vertical transversely isotropic (VTI) media. We discuss a multiparameter acoustic VTI inversion for P-wave velocity and the anisotropy parameter epsilon. Furthermore, we include well logs as constraints to help stabilize the inversion and provide us with more reliable velocity updates. In the next section, we include attenuation and dispersion effects to better simulate wave propagation through real Earth materials. We present a visco-acoustic WFI for updating both the velocity model and the quality factor (Q) in a recursive mode. We illustrate these approaches on applications to real 3D data.

Introduction

Waveform inversion (WFI) is a seismic method for deriving high-fidelity Earth models for seismic imaging by minimizing a misfit function of the difference between the measured and modeled data. WFI was first introduced by Lailly, Tarantola, and Mora using a gradient-based iterative algorithm (Lailly, 1983; Tarantola, 1984, 1987, 1988; Mora, 1987, 1988). Since these pioneering efforts, many researchers have attempted to use various strategies and computational schemes to make WFI, whether implemented in the time or frequency domain, a processing tool for real data sets (e.g., Sirgue and Pratt, 2004; Shin and Min, 2006; Vigh and Starr, 2006; Operto et al., 2007). An excellent technical review of WFI is given in Virieux and Operto (2009).

The basic physics of the problem is easily understood. Here, we will purposely avoid the use of complex formulas and instead focus on the physically intuitive concepts. We refer the interested reader to the references for technical details.

The basic premise of WFI is that the model describing the subsurface, i.e., velocity, density, anisotropy, and attenuation of the rocks in the Earth, can be obtained by minimizing the difference between data generated by surface seismic sources and recorded at surface receivers and the synthetic data generated using these sources and receivers locations and creating the wavefields with computers. To generate these wavefields, one needs wave equations that simulate the propagation of waves in the Earth. So one assumes a model of the Earth, and using this model, however complex, simulates what he or she should see at the receivers for each source. The simulated data will obviously not match the recorded data, as the model is sure to be wrong. However, by using the deviations of the modeled data from the real data, we seek to correct the model. To that end, suppose that one knows a priori how the synthetic data change given a small change in the model. Obviously the real data will not change. The trick then is to go backward, namely given a wanted change in the surface synthetic data what part of the model do we need to change so that the simulated data get closer to the observed data? This is where the "magic" of adjoint-state methods comes in (Plessix, 2006). They tell us to propagate the change we wish to have at the surface backward into the Earth in an acausal way. This backward propagation tells us effectively how to change the model in the subsurface; i.e., which direction to make the change. We try a small change in that direction, recreate the predicted data at the surface again, and recompute the difference. By repeating this process, the model is updated using this iterative method for nonlinear optimization.

WFI is a highly nonlinear, ill-posed optimization problem as we described heuristically earlier. We introduce additional "geological or geophysical" information and turn the unconstrained optimization problem into a constrained optimization problem in order to reduce the ill-posedness. The geological settings and the geophysics of the problem lead to appropriate constraints, such as restriction of smoothness or sharpness of model parameters, or information from well logs. In this article, we use well logs as constraints (providing an absolute velocity scale) and solve the WFI problem using an augmented Lagrangian method (ALM), a popular method essentially equivalent to a minimization problem with constraints using Lagrange multipliers, that replaces a constrained optimization problem by a series of unconstrained problems. The unconstrained objective function is the Lagrangian of the constrained problem, with an additional penalty term (the augmentation). The ALM with well constraints provides a more useful and reliable recovery of velocity profiles from well logs and seismic data including a better delineation of velocity at or close to well locations. Regularization techniques such as total variation regularization or Tikhonov regularization are also beneficial for the solution of this problem (Wang et al., 2012).

The quality of WFI critically depends on the adequacy of the forward-modeling wave equations and of the adjoint equations to correctly represent the physics for all the waves

during WFI iterations. Depending on the characteristics and property of the physical media, various wave equations have been applied for different scenarios. The inclusion of anisotropy is kinematically necessary and often helps to improve WFI results for media with strong anisotropy. The compensation of anelastic behavior cannot be ignored for physical materials with strong attenuation such as gas clouds. In this article, we mainly discuss the effects of including anisotropy and attenuation for WFI.

In the first section of this article, forward modeling and its adjoint are computed based on acoustic-wave equations in vertical transversely isotropic (VTI) media. For anisotropic media, anisotropic WFI provides a more reliable subsurface reconstruction of structures than isotropic WFI, because it more properly models the kinematics of wave propagation in real materials. We propose a joint inversion for both the P-wave velocity model and the Thomsen anisotropy parameter model. In this section, we will also investigate how to include well constraints to stabilize the results of WFI.

In the second section, we discuss the effects of attenuation on WFI. Viscoelasticity provides a powerful tool to model real Earth materials (Robertsson et al., 1994). In a viscoelastic model, viscoelastic relaxation functions are applied. A superposition of standard linear solids (SLS) in parallel is controlled by a set of relaxation parameters to simulate the attenuation and dispersion effects that the real Earth materials have on wave propagation. The relaxation parameters can be obtained from certain relationships between the quality factor Q and frequency to approximate a specific viscoelastic model (Blanch et al., 1995). In many applications, a single SLS suffices to compensate for the anelastic behavior. Viscoelastic wave equations have been implemented using finite-difference wavefield extrapolation on staggered girds. (Robertsson et al., 1994; Larsen and Grieger, 1998). In this article, we limit our work to visco-acoustic media. In order to compensate for the attenuation effects in WFI, visco-acoustic relaxation functions are applied with only one SLS.

For both sections, wavefields are generated using high-order finite-difference schemes on centered grids.

We will illustrate how WFI performs using results for a 3D real ocean-bottom-cable (OBC) data set from the Green Canyon area of the Gulf of Mexico.

Anisotropic WFI

Assuming that the shear velocity is zero, we can derive VTI acoustic-wave equations that kinematically model, the compressional wave propagation. Based on Alkhalifah (2000)'s pseudo-acoustic approximation, a number of variations of pseudo-acoustic-wave equations have been developed (Zhou, 2006). Here we use a VTI system of two coupled second-order partial differential equations in terms of P-wave vertical velocity, and the Thomsen anisotropy parameters epsilon and delta.

Having computed the forward-propagated wavefields based on the acoustic VTI wave equations, we modify the traditional misfit function (Tarantola, 1987) slightly and add well constraints:

$$\min_{m} \quad J[m] = \left\| \mathbf{T}(d_0 - \varsigma d) \right\|_2^2$$
$$s.t. \quad \mathbf{P}m = m_0,$$

where $d_0 = d_0(\mathbf{x}_r, t; \mathbf{x}_s)$ is the observed seismic data and $d = d(\mathbf{x}_r, t; \mathbf{x}_s)$ is the predicted data for the model m at source and receiver locations, $\mathbf{x}_s$ and $\mathbf{x}_r$. The predicted data are obtained by sampling the extrapolated wavefield generated by a high-order finite difference scheme to the receiver locations, based on the acoustic VTI wave equations. $\mathbf{T}$ is a data preconditioner and ς is a normalization scalar. The target model can be parameterized by any appropriate model describing the subsurface properties. In this article, we use the P velocity model and the epsilon model for the anisotropic WFI. m_0 is the model generated from well logs. $\mathbf{P}$ is the projection operator that maps the model m to m_0's grid.

This problem can be solved as an unconstrained minimization problem using ALM (Hestenes, 1969; Powell, 1969; Li, 2011):

$$\min_{m} J_A[m] = \frac{1}{2}\left\| \mathbf{T}(d_0 - \varsigma d) \right\|_2^2 - \langle \lambda, \mathbf{P}m - m_0 \rangle + \frac{\mu}{2}\left\| \mathbf{P}m - m_0 \right\|_2^2,$$

where λ is a Lagrange multiplier and μ is a penalty scalar. The major advantage of the method is that unlike the penalty method, it is not necessary to take $\mu \to \infty$ in order to solve the original constrained problem. It uses the gradient at an initial point for an initial direction estimate and updates that direction using a nonlinear conjugate gradient method or limited-memory Broyden-Fletcher-Goldfarb-Shanno (L-BFGS) method that takes advantage of the approximate Hessian inverse. The gradients with respect to the velocity and epsilon are computed by solving the adjoint equations of the acoustic VTI equations and crosscorrelating the proper back-propagated wavefields by back-propagating the residual with the forward-propagated wavefields.

Convergence can be accelerated using gradient preconditioning. The current preconditioning normalizes the gradient by the amplitude of the forward propagated wave with a whitening factor. We also apply layer stripping and/or masking as another gradient preconditioning tool to accelerate the convergence.

Visco-acoustic WFI

In visco-acoustic media, the forward-propagated wavefield can be obtained by the relationship between pressure and particle velocity for a single SLS (Robertsson et al., 1994). A single SLS consists of a spring in parallel with a spring and a dashpot in series to model the behavior of a viscoelastic material. In a single SLS, the stress-strain relationship is expressed as a causal time convolution of a stress relaxation function with the strain rate. This time dependence of the relaxation mechanism is governed by stress and strain relaxation times, which describe the physical dissipation mechanism that the real Earth materials have on wave propagation. The relaxation times can be obtained from the quality factor Q given a reference frequency according to Blanch et al. (1995). Finite-difference methods on staggered grids are commonly used to extrapolate the forward-propagated wavefield.

In order to eliminate the convolution in the original visco-acoustic-wave equation, we introduce a memory variable, derive a first-order linear differential equation for it, and update it by a recursive convolution method (Bai and Yingst, 2013).

Based on the properties of the modified visco-acoustic equation, we can verify that the corresponding memory variable in its adjoint equation is the history of pressure and is responsible for the anelastic behavior. This memory variable is governed by a time convolution of pressure with an exponential function, which is the relaxation function. The kernel of this memory variable is of exponential character too. Energy now increases with time compensating for the attenuation effects in backward propagation.

We calculate the two memory variables on the same grids as used for the wavefield. As a result, the visco-acoustic WFI is implemented by high-order finite-difference methods on centered grids instead of on staggered grids. This significantly reduces computation time and memory requirements.

Example of anisotropic WFI

The first example is an application of joint VTI WFI with well constraints to 3D marine data. This deep water OBC survey is located in the Green Canyon area of the Gulf of Mexico. The acquisition area was 160 km^2 and used four-component OBC equipment in deep water (1000+ m) over relatively shallow salt bodies with 19,901 shots. Each shot has 239 receivers. The data with offset range from 3000–7000 m are used and the frequencies used range from 2 to 10 Hz. The source signature is derived from the down-going wavefield on a zero-offset section.

The sensitivity analysis of acoustic anisotropic WFI has shown that the seismic data are more sensitive to the velocity perturbation and the anisotropy parameter epsilon than the anisotropy parameter delta. Therefore our target models were parameterized by P-wave velocity and the anisotropy parameter epsilon, while delta was kept unchanged over WFI iterations. The initial models for WFI, Figures 1a and 2a, were built from anisotropic VTI ray-based tomographic inversions.

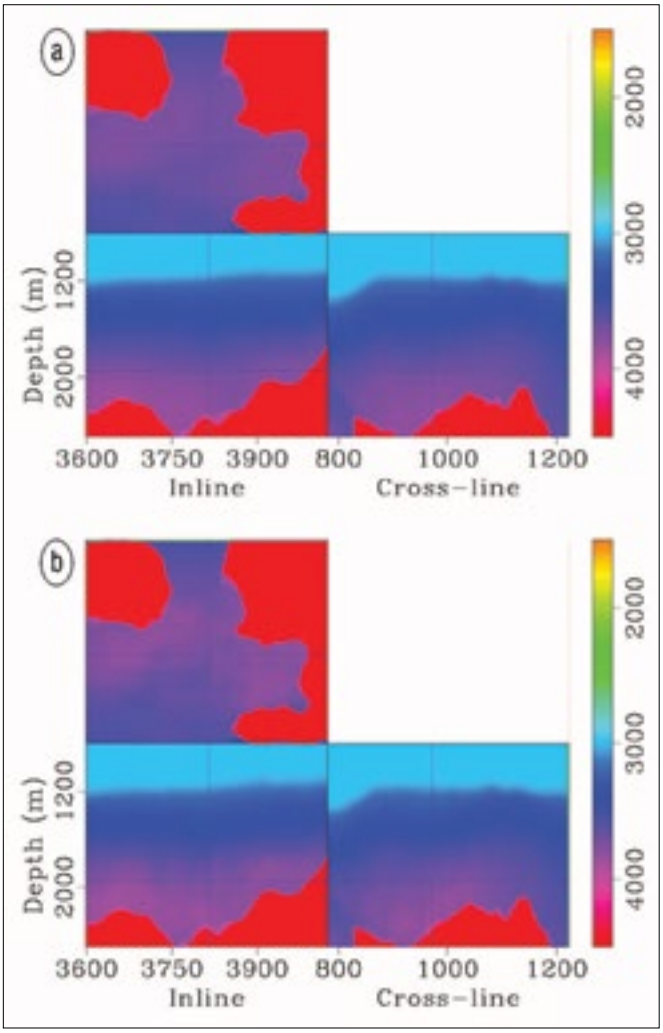

Figure 1. *(a) Initial velocity model before anisotropic WFI. (b) Updated velocity model after anisotropic WFI. Upper left = depth slice, lower left = inline slice, lower right = crossline slice.*

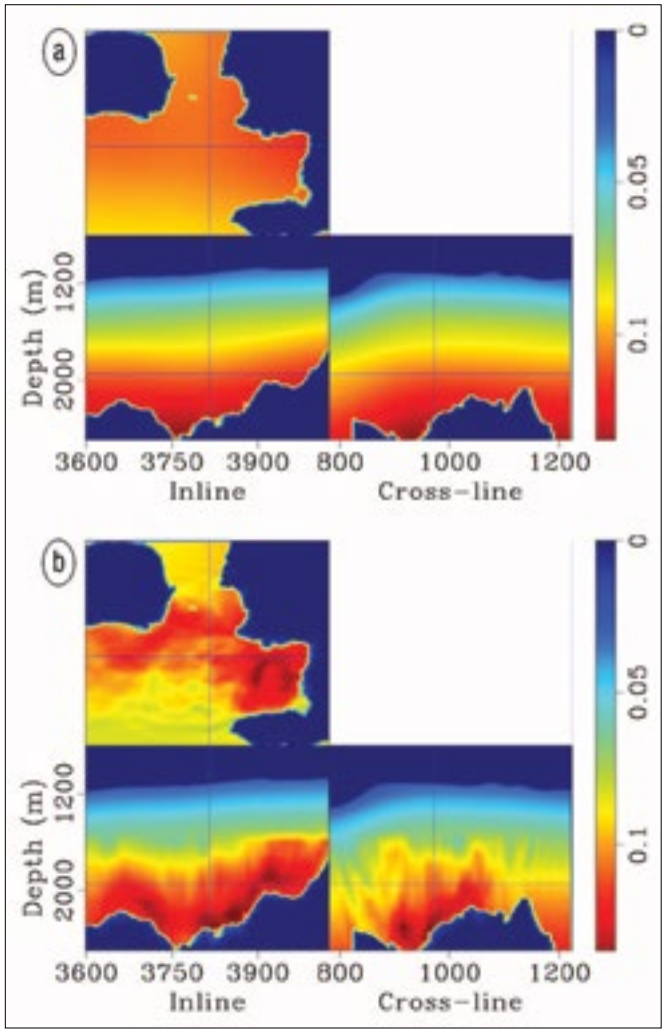

Figure 2. *(a) Initial epsilon model before anisotropic WFI. (b) Updated epsilon model after anisotropic WFI. Upper left = depth slice, lower left = inline slice, lower right = crossline slice.*

Delivering innovative technologies for complex geologies.

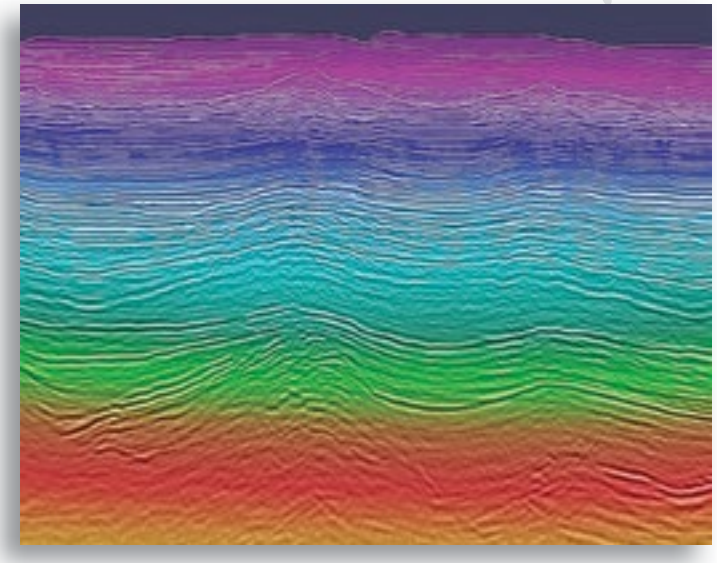

Velocity model before application of general moveout tomography.

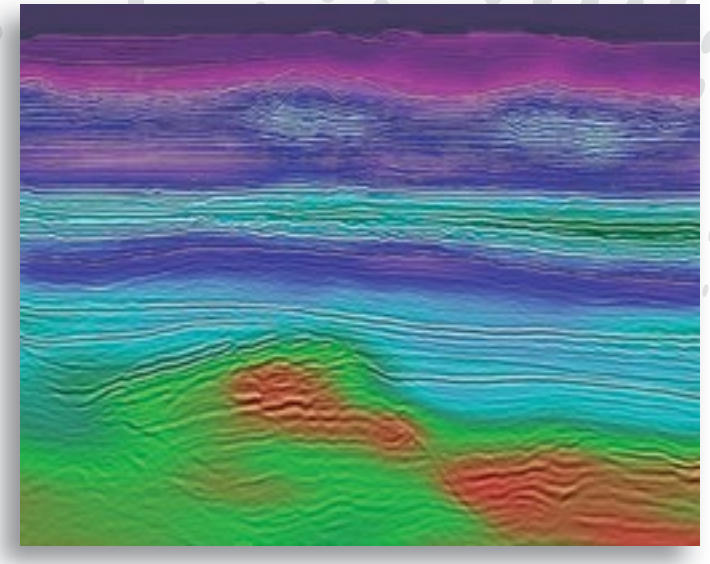

Application of GX Technology's high resolution tomography using accurate general moveout picks resolves small-scale velocity heterogeneities.

Since introducing the industry-leading RTM and 3D SRME solutions, ION's GX Technology (GXT) group has continued its pioneering research efforts to develop innovative, advanced imaging technologies. Leveraging techniques ranging from extending low frequencies with WiBand™ broadband processing, to generalized moveout (GMO) picking for tomography, as well as advanced waveform inversion (WFI), GXT offers fit-for-purpose, ray- or wave-based, fine-scale velocity modeling. Your result? Superior high resolution images for complex geologies to improve exploration and production success. To learn more, visit iongeo.com/imagingleaders.

AREAS OF EXPERTISE

Unconventional Reservoirs

Challenging Environments

→ **Complex Geologies**

Basin Exploration

Reservoir Exploitation

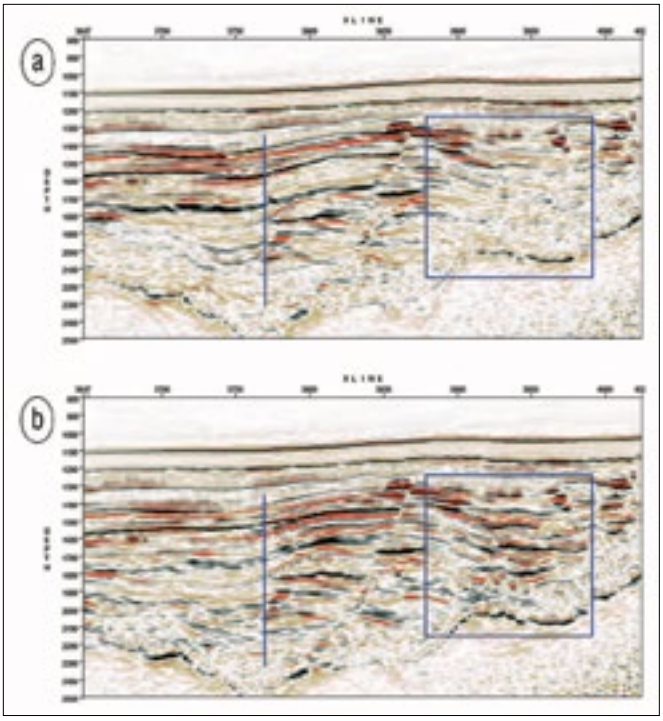

Figure 3. *(a) Stack image using the initial velocity model and the initial epsilon model before anisotropic WFI. (b) Stack image using the updated velocity model and the updated epsilon model after anisotropic WFI.*

Various strategies, such as multiscale, layer stripping, and offset weighting are quite useful to minimize the risk of converging to local minima. We applied multiscale inversion, gradually increasing the frequency bandwidth to avoid the cycle-skipping issue. We also applied layer stripping, inverting successively deeper layers using the presumably correct velocity model in shallower layers to speed up the convergence. The inversion also proceeded with spectral shaping applied to the field data and the source wavelet for accelerating convergence. Source delay time and offset weights were automatically computed.

For the joint anisotropic WFI, we used a fixed delta model and constant density (ρ = 1 g/cm^3). We first fixed the epsilon model (Figure 2a) and updated the velocity. The inverted velocity model in Figure 1b after 10 iterations shows reasonable shallow updates up to a depth of approximately 2000 m including some detailed structures above the salt. Although not shown here in detail, the velocity profiles were much improved by adding the well-log constraints. Next, we started from the updated velocity (Figure 1b) and initial epsilon model. The velocity model was kept unchanged, and our goal was to update the epsilon model. The inverted epsilon model in Figure 2b after 10 iterations shows reasonable shallow update as well. To further evaluate the anisotropic WFI results, we generated stack images with the initial models and the inverted models obtained by WFI. The stack image after the WFI iterations (shown in Figure 3b for inline 976) shows remarkable improvement compared to the initial stack (shown in Figure 3a) with better focus and event consistency, especially in the blue squared area. Apparent faulting is visible

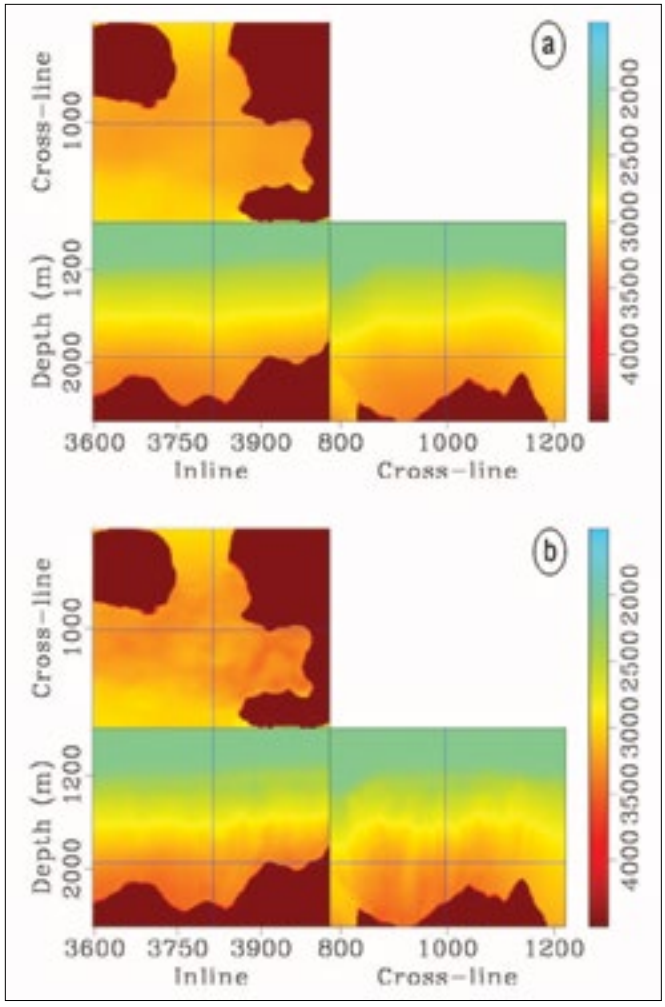

Figure 4. *(a) Initial velocity model before visco-acoustic WFI. (b) Updated velocity model after visco-acoustic WFI. Upper left = depth slice, lower left = inline slice, lower right = crossline slice.*

in the event package in the blue square. Well location is also displayed using blue lines on Figure 3.

Example of visco-acoustic WFI

The second example is visco-acoustic WFI applied to the same data set. We first perform visco-acoustic WFI to estimate a Q model from a constant Q model (Q = 5000), using the same source wavelet, the initial isotropic-velocity model, and constant density (ρ = 1 g/cm^3). After a Q model is obtained, we invert for the velocity model in Figure 4b using the initial velocity model in Figure 4a and the updated Q model in Figure 5. The main geological structures imaged with the initial velocity model, without the benefit of incorporating any waveform inversion, are shown in Figure 6a. The structures in this zoomed-in area of interest for inline 972 are poorly imaged. The corresponding Q model shown in Figure 5 indicates strong attenuation in the area of interest. The energy is much better focused in Figure 6b, which is obtained from the inverted velocity model with attenuation. The image resolution is greatly improved by using the velocity determined with the visco-acoustic waveform inversion. It should be noted that we are using an iterative procedure,

where we start with an initial velocity model, from which we obtain a Q model through an inversion step, and then iterate. In the field data example that we have shown, only a second velocity inversion was needed after the Q determination. This is because the initial model was already accurate, something which does not always occur in practice. Because the velocity update mostly affects the phase of the data, and the Q update mostly affects the amplitude of the data, convergence seems to happen rapidly, although we have not investigated that issue in detail.

Conclusions

We presented a methodology and strategies for WFI with well constraints, anisotropy, and attenuation. Including anisotropy and attenuation provides more accurate wavefield models and therefore helps to improve the WFI results. Including well constraints help to stabilize the inversion. These approaches were illustrated on a 3D marine data set from the Green Canyon area of the Gulf of Mexico. From the WFI results, we showed that WFI including well constraints, anisotropy, and attenuation has the potential to provide us with more useful and reliable model updates. TLE

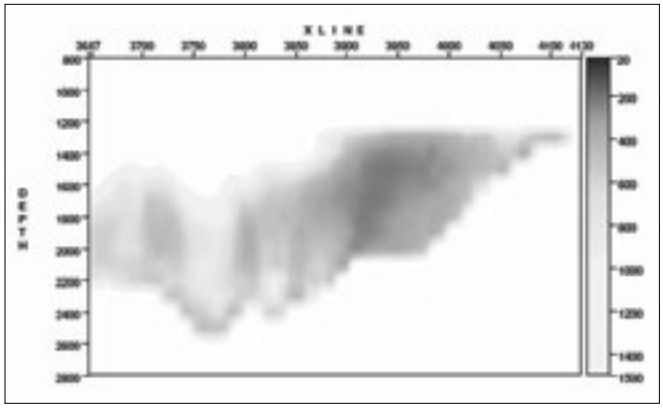

Figure 5. *Updated Q model after visco-acoustic WFI.*

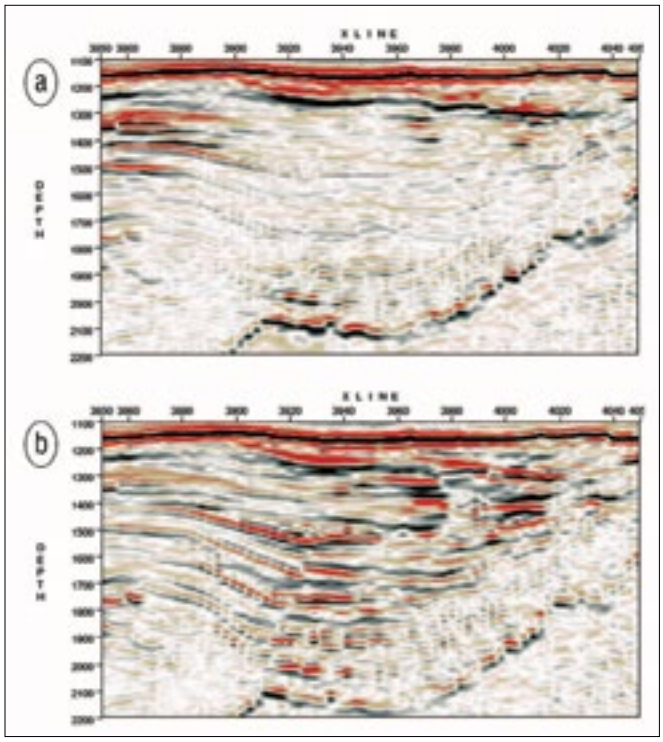

Figure 6. *(a) Initial stack image before visco-acoustic WFI. (b) Updated stack image after visco-acoustic WFI.*

References

Alkhalifah, T., 2000, An acoustic wave equation for anisotropic media: Geophysics, **65**, no.4,1239–1250,http://dx.doi.org/10.1190/1.1444815.

Bai, J. and D. Yingst, 2013, Q estimation through waveform inversion: 75th Conference and Exhibition, EAGE, Extended Abstracts.

Blanch, J. O., J. O. A. Robertsson, and W. W. Symes, 1995, Modeling of a constant Q: Methodology and algorithm for an efficient and optimally inexpensive viscoelastic technique: Geophysics, **60**, no. 1, 176–184, http://dx.doi.org/10.1190/1.1443744.

Hestenes, M., 1969, Multiplier and gradient methods: Journal of Optimization Theory and Applications, **4**, 303–320.

Lailly, P., 1983, The seismic inverse problem as a sequence of before-stack migrations: *in* J. Bednar, E. Robinson, A. Weglein, eds. Conference on Inverse Scattering, Theory and Applications, Society for Industrial and Applied Mathematics, 206–220.

Larsen, S. and J. Grieger, 1998, Elastic modeling initiative, part III: 3-D computational modeling: 68th Annual International Meeting, SEG, Expanded Abstracts, 1803–1806.

Li, C., 2011, Compressive sensing for 3D data processing—a unified method and its applications: PhD thesis, Rice University.

Liu, H.-P., D. L. Anderson, and H. Kanamori, 1976, Velocity dispersion due to anelasticity; implications for seismology and mantle composition: Geophysical Journal of the Royal Astronomical Society, **47**, no. 1, 41–58, http://dx.doi.org/10.1111/j.1365-246X.1976.tb01261.x.

Mora, P., 1987, Nonlinear two-dimensional elastic inversion of multioffset seismic data: Geophysics, **52**, no. 9, 1211–1228, http://dx.doi.org/10.1190/1.1442384.

Mora, P., 1988, Elastic wave-field inversion of reflection and transmission data: Geophysics, **53**, no. 6, 750–759, http://dx.doi.org/10.1190/1.1442510.

Operto, S., J. Virieux, P. Amestoy, J. l'Excellent, L. Giraud, and H. Ali, 2007, 3D finite-difference frequency-domain modeling of visco-acoustic wave propagation using a massively parallel direct solver: A feasibility study: Geophysics, **72**, no. 5, SM195–SM211, http://dx.doi.org/10.1190/1.2759835.

Plessix, R.-E., 2006, A review of the adjoint-state method for computing the gradient of a functional with geophysical applications: Geophysical Journal International, **167**, no. 2, 495–503, http://dx.doi.org/10.1111/j.1365-246X.2006.02978.x.

Powell, M., 1969, A method for nonlinear constraints in minimization problems: Academic Press, New York, NY, 283–298.

Robertsson, J. O. A., J. O. Blanch, and W. W. Symes, 1994, Viscoelastic finite-difference modeling: Geophysics, **59**, no. 9, 1444–1456, http://dx.doi.org/10.1190/1.1443701.

Shin, C. and D. Min, 2006, Waveform inversion using a logarithmic wavefield: Geophysics, **71**, no. 3, R31–R42, http://dx.doi.org/10.1190/1.2194523.

Sirgue, L. and R. Pratt, 2004, Efficient waveform inversion and imaging: A strategy for selecting temporal frequencies: Geophysics, **69**, no. 1, 231–248, http://dx.doi.org/10.1190/1.1649391.

Tarantola, A., 1984, Inversion of seismic reflection data in the acoustic approximation: Geophysics, **49**, no. 8, 1259–1266, http://dx.doi.org/10.1190/1.1441754.

Tarantola, A., 1987, Inverse problem theory: Elsevier.

Tarantola, A., 1988, Theoretical background for the inversion of seismic waveforms, including elasticity and attenuation: Pure and Applied Geophysics, **128**, no. 1–2, 365–399, http://dx.doi.org/10.1007/BF01772605.

Thomsen, L., 1986, Weak elastic anisotropy: Geophysics, **51**, no. 10, 1954–1966, http://dx.doi.org/10.1190/1.1442051.

Vigh, D. and E. Starr, 2006, Shot profile versus plane wave reverse time migration: 76th Annual International Meeting, SEG, Expanded Abstracts, 2358–2361.

Virieux, J. and S. Operto, 2009, An overview of full-waveform inversion in exploration geophysics: Geophysics, **74**, no. 6, 127–152, http://dx.doi.org/10.1190/1.3238367.

Wang, C., D. Yingst, R. Bloor, and J. Leveille, 2012, Application of VTI waveform inversion with regularization and preconditioning to real 3D data: 74th Conference and Exhibition, EAGE, Extended Abstracts.

Zhou, H., G. Zhang, and R. Bloor, 2006, An anisotropic wave equation for vti media: 68th Conference and Exhibition, EAGE, Extended Abstracts.

Acknowledgments: We thank ION-GXT for permission to use the data set and to publish the results. We also thank our colleagues at ION R&D and GAG for providing us valuable support in this work, especially Ian Jones, Helen Delome, Carlos Calderon, Milos Cvetkovic, Mick Surgue, Stuart Greenwood, Joe Zhou, Guoquan Chen, and Herman Jaramillo.

Corresponding author: chao.wang@iongeo.com